ChemPubSoc Europe

DOI: 10.1002/chem.201602992

CHEMISTRY
A European Journal
Full Paper

Organocatalysis | *Hot Paper*

Enantioselective Organocatalytic Cascade Approach to Different Classes of Benzofused Acetals

Bruno Matos Paz, Lydia Klier, Line Næsborg, Vibeke Henriette Lauridsen, Frank Jensen, and Karl Anker Jørgensen*[a]

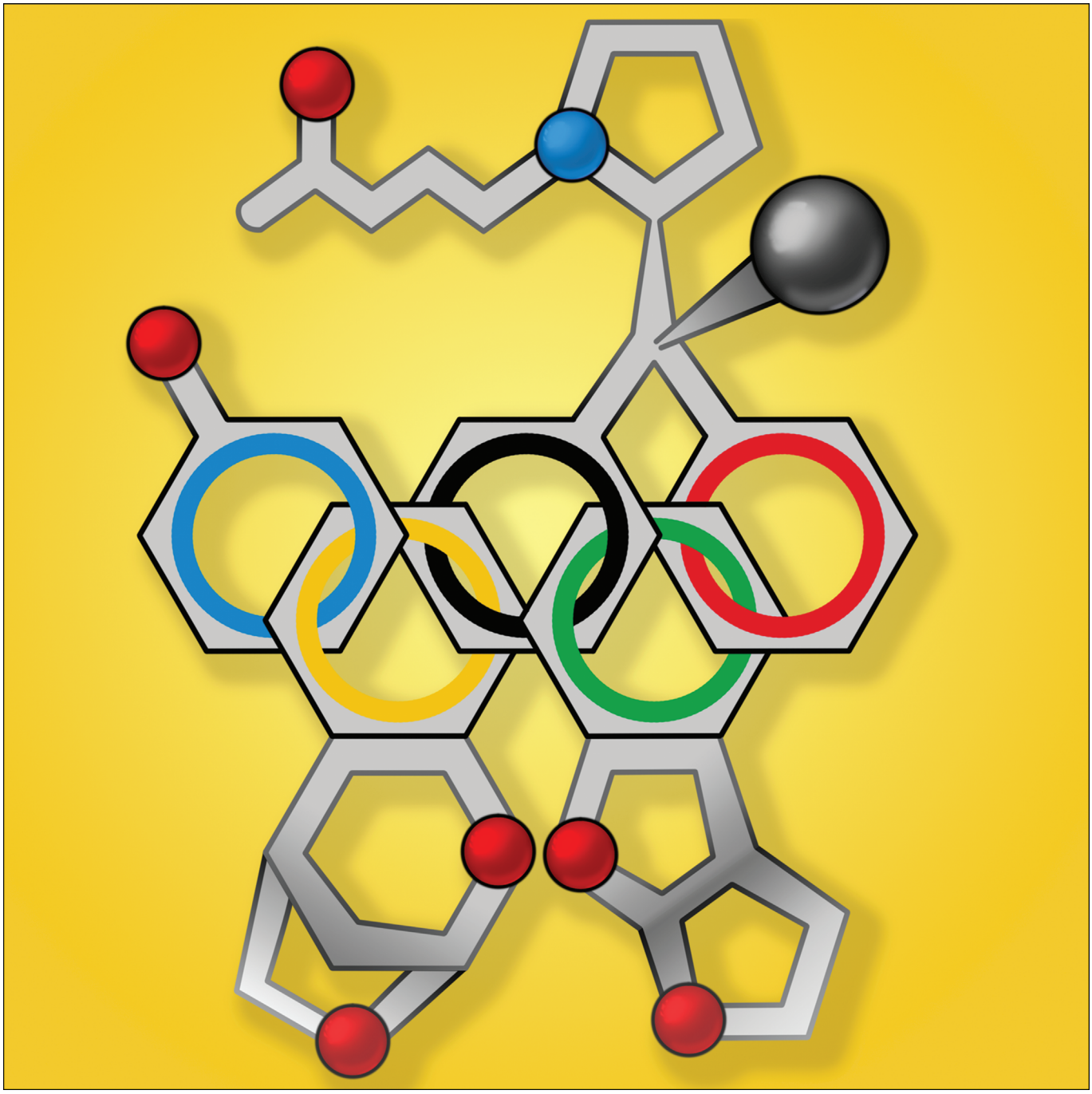

Abstract: A novel enantioselective organocatalytic strategy is presented for the synthesis of tetrahydrofurobenzofuran and methanobenzodioxepine natural product core structures. The strategy is based on a pair of divergent reaction pathways in which hydroxyarenes react with γ-keto-α,β-unsaturated aldehydes, catalyzed by a chiral secondary amine. One reaction pathway, which leads to chiral 5,5-fused acetals with two stereocenters—the tetrahydrofurobenzofuran scaffolds—proceeds in moderate yields and up to 96% *ee*. The other reaction pathway provides 5,6-bridged methanobenzodioxepine scaffolds with three stereocenters in moderate to good yields and up to 95% *ee*. The reaction is remarkable as it can proceed with catalyst loadings as low as 0.25 mol%, providing one of the highest known turnover numbers in iminium ion catalysis. Furthermore, the hemiacetal tetrahydrofurobenzofuran can undergo functionalizations including reduction, oxidation, and allylation. Finally, the effects involved in the substrate control for the divergent pathways, based on both experimental and computational studies, have been investigated. A model involving steric, electronic and stereoelectronic interactions is discussed to rationalize the observed selectivities.

Introduction

Chiral fused, bridged, and spirocyclic acetals are widespread in nature.[1] The bioactivity of these compounds is often dependent on the substituent pattern and stereochemistry of the acetal functionality, which has motivated numerous efforts towards the development of concise stereoselective syntheses of such acetals.[2]

Restricting attention to benzofused acetals, some of these natural compounds and their synthetic analogues possess a wide range of biological activities. Whereas aflatoxins (Figure 1, **A**), widespread food contaminants, are toxic and carcinogenic mycotoxins,[3] other highly desirable antimicrobial, antifungal, anti-HIV, and anticancer properties are found in related benzofused acetal scaffolds (Figure 1, **C**).[4]

Since pioneering works by the groups of Büchi and Roberts,[5] several racemic synthetic endeavors have been developed for the construction of the tetrahydrofurobenzofuran system present in aflatoxins (Figure 1, **A**).[6] However, more recently, enantioselective approaches aiming for the natural product synthesis of the tetrahydrofurobenzofuran scaffold have been put forward. These strategies have relied on the use of chiral Lewis acid catalysis for the activation of *para*-quinones[7] or palladium-catalyzed acetalization followed by reductive Heck coupling.[8] The first strategy restricted the substitution pattern of the aromatic moiety, whereas the second relied on prefunctionalization of the hydroxyarenes used, and both were mainly limited to hydrogen substituents on the acetal moiety.[9]

In striking contrast to the tetrahydrofurobenzofuran core, the methanobenzodioxepine scaffold, present in bullataketals (Figure 1, **B**), has received little attention and no enantioselective synthesis of this scaffold has been reported to date.[10] Furthermore, the tetrahydrofurobenzofuran and methanobenzodioxepine scaffolds are both present in butyrylcholinesterase inhibitors with potential use in the treatment of neurodegenerative diseases such as Alzheimer's disease.[11]

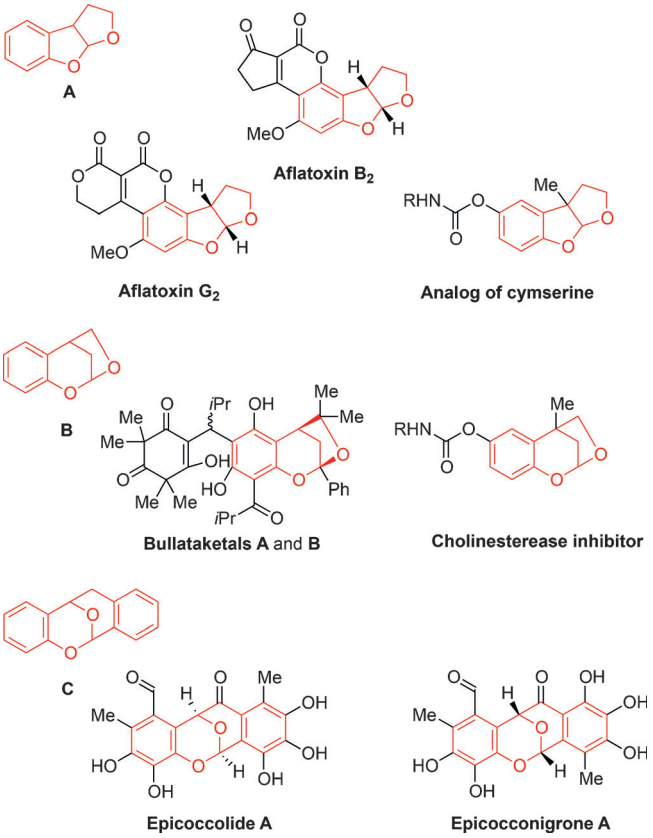

Figure 1. Biologically active compounds containing benzofused acetal scaffolds.

Driven by the intriguing structural complexity and remarkable biological properties of the tetrahydrofurobenzofuran and methanobenzodioxepine scaffolds, we decided to investigate the feasibility of enantioselective organocatalytic divergent pathways for the synthesis of these scaffolds. The present strategy is based on the hypothesis that an iminium ion-catalyzed reaction between hydroxyarenes and γ-keto-α,β-unsaturated aldehydes (γ-keto-enals) could give access to both scaffolds in an enantioselective fashion, by means of a Friedel–

[a] *B. M. Paz, Dr. L. Klier, L. Næsborg, V. H. Lauridsen, Prof. Dr. F. Jensen, Prof. Dr. K. A. Jørgensen*
Department of Chemistry, Aarhus University
DK-8000 Aarhus C (Denmark)
E-mail: kaj@chem.au.dk

Supporting information for this article can be found under: http://dx.doi.org/10.1002/chem.201602992.

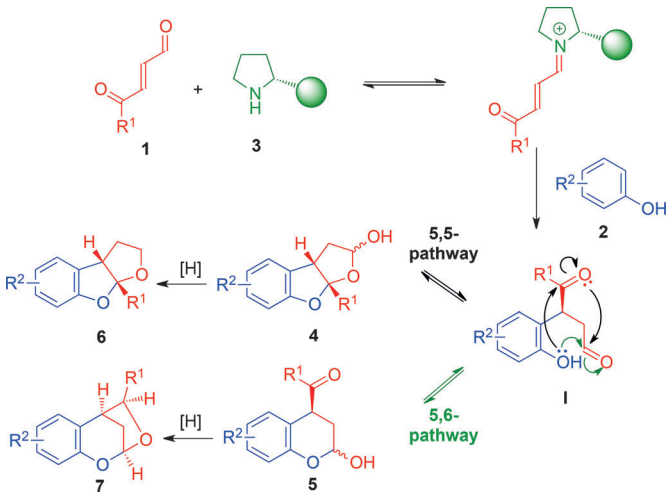

Scheme 1. Iminium ion-catalyzed formation of benzofused acetals: tetrahydrofurobenzofuran (**6**) and methanobenzodioxepine (**7**) scaffolds.

Crafts reaction[12] followed by an acetalization cascade (Scheme 1).

The two different reaction products are formed through a pair of divergent pathways from the same classes of starting compounds. The first path (Scheme 1, **I**; black arrows) leads to a chiral 5,5-fused acetal bearing two stereogenic centers, including a quaternary center, whereas the second (Scheme 1, **I**; green arrows) provides a 5,6-bridged product with three stereocenters. Given the usually low turnover numbers of organocatalyzed reactions, a further development presented is the use of low catalyst loadings, and the use of commercially available hydroxyarenes as nucleophiles. Finally, we have also integrated a series of experimental and computational studies in an attempt to account for the origins of a remarkable influence of substrate control in the product distribution.

Results and Discussion

The reaction between γ-keto-enal **1a** and 1-naphthol **2a** was used as model to test our hypothesis. When diarylprolinol silyl ether **3a**[13] was applied as the catalyst (10 mol%), to our delight, full conversion was rapidly obtained (Table 1). However, the products were formed as a mixture of epimers of hemiacetals **4a** and **5a**. Upon reduction with $BF_3{\cdot}OEt_2/HSiEt_3$, product **6a** was obtained as the major product, together with **7a** as the minor product. To optimize the reaction conditions for the formation of tetrahydrofurobenzofuran **6a** (5,5-reaction path, Scheme 1), the influence of various reaction parameters was investigated. Full conversion was observed in 2 h in the absence of acid; however, the isolated product **6a** was formed in lower enantioselectivity (Table 1, entry 1; 60% *ee*). By applying pivalic acid, full conversion was observed in <1 h, albeit with an almost equally low enantioselectivity (Table 1, entry 2; 62% *ee*). When benzoic acid was applied as a cocatalyst, the enantioselectivity was increased to 76% *ee*. By testing benzoic acids with different substituent patterns,[14] *ortho*-nitrobenzoic acid proved to be the best and **6a** was formed with 94% *ee*

Table 1. Optimization of solvent and acid cocatalyst for the formation of tetrahydrofurobenzofurans.[a,b]

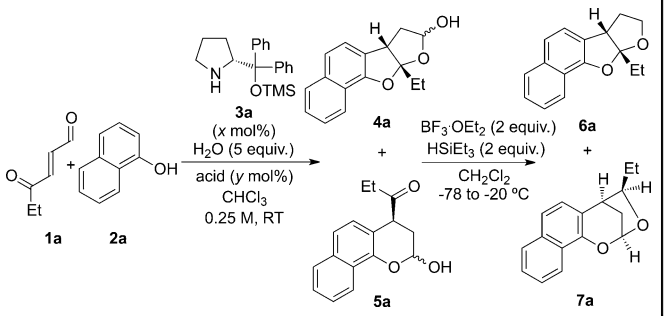

Entry	Cat. [mol%]	Cocat. [mol%]	Acid cocat.	*t* [h][b]	*ee*[c] [%]
1	10	–	–	2	60
2	10	10	$tBuCO_2H$	<1	62
3	10	10	$PhCO_2H$	<1	76
4	10	10	$o\text{-}NO_2C_6H_4CO_2H$	<1	94
5	2.5	10	$o\text{-}NO_2C_6H_4CO_2H$	3	94
6	1	1	$o\text{-}NO_2C_6H_4CO_2H$	6	87
7	0.5	0.5	$o\text{-}NO_2C_6H_4CO_2H$	24	85
8	0.5	2.5	$o\text{-}NO_2C_6H_4CO_2H$	15	92
9	0.5	5	$o\text{-}NO_2C_6H_4CO_2H$	15	93
10	0.5	10	$o\text{-}NO_2C_6H_4CO_2H$	15	94

[a] Reactions were performed on a 0.1 mmol scale, with 1.2 equivalents of 1-naphthol; [b] full conversion (>95%) was determined by ^1H NMR spectroscopy of the crude reaction mixture; [c] determined by chiral stationary phase chromatography (UPC^2) for **6a**.

(Table 1, entry 4). For each reaction screened, 5 equivalents of water were applied since, in the absence of water, no product formation was observed.

The short reaction times (<1 h) prompted us to investigate the influence of catalyst and acid cocatalyst loadings (Table 1, entries 5–10). By reducing the catalyst loading to 2.5 mol%, full conversion into **6a** was obtained in 3 h, without loss of enantioselectivity (Table 1, entry 5; 94% *ee*). However, a drop in enantioselectivity of **6a** was observed when catalyst and acid loadings were simultaneously reduced (Table 1, entries 6 and 7). The optimal compromise between reaction time and selectivity was obtained by applying a catalyst loading of 0.5 mol% and an acid loading of 10 mol% (Table 1, entry 10; 94% *ee*). Lower catalyst loadings led to very long reaction times (>48 h). Higher acid loadings did not reduce the reaction time or improve the enantioselectivity, but provided an increased amount of unidentified byproducts (results not shown). With the final conditions in hand, we decided to explore the two reaction pathways.

To understand the nature and extension of substrate control for the 5,5 and 5,6 reaction pathways (Scheme 1) leading to the tetrahydrofurobenzofuran **6** and methanobenzodioxepine **7** scaffolds, respectively, the influence of the R^1 substituent on the γ-keto-enals was investigated. The ratio between **6** and **7** is postulated to be dependent on the relative amounts of hemiacetals **4** and **5**, which are in equilibrium via intermediate **I** (Scheme 1). As the mixture of four isomers rendered impractical the direct measurement of the equilibrium ratio between **4** and **5** prior to reduction, an indirect measurement was used

Table 2. Substrate control for the formation of **6** and **7**.[a]

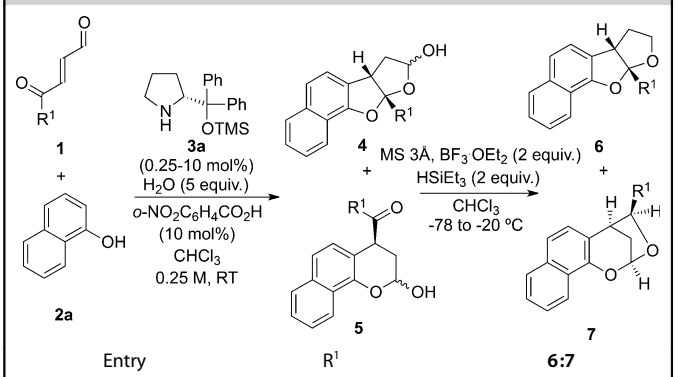

Entry	R^1	6:7
1	CH_3 (**1b**)	2.3:1
2	CH_2CH_3 (**1a**)	9:1
3	$CH(CH_3)_2$ (**1c**)	>20:1
4	$C(CH_3)_3$ (**1d**)	>20:1
5	CH_2Ph (**1e**)	9:1
6	CH_2CH_2Ph (**1f**)	>20:1
7	$CH_2(CH_2)_3CH_3$ (**1g**)	3.3:1
8	Ph (**1h**)	1:>20
9	*p*-CNC_6H_4 (**1i**)	1:4.5
10	*p*-$NO_2C_6H_4$ (**1j**)	1.2:1

[a] Ratios were determined by ^{1}H NMR spectroscopy of the crude reaction mixture after the reduction step. For product **6**, the ratio also includes the amount of a benzofuran byproduct.[14]

instead, based on the ratios of the reduced products **6** and **7** (Table 2).[14]

The product distribution providing the tetrahydrofurobenzofuran **6** and methanobenzodioxepine **7** scaffolds is highly dependent on the R^1 substituent in the γ-keto-enal **1** (Table 2). For $R^1 = CH_3$, the reaction shows a small preference towards the formation of **6b** (Table 2, entry 1), whereas for $R^1 = CH_2CH_3$ product **6a** is formed with a 9:1 selectivity relative to **7a** (Table 2, entry 2). With more sterically demanding groups in the aldehyde side-chain ($R^1 = CH(CH_3)_2$ and $C(CH_3)_3$), the selectivity of the reaction changes exclusively to **6c** or **6d** (Table 2, entries 3 and 4; >20:1). In the presence of a benzyl group ($R^1 = CH_2Ph$), the selectivity towards **6e** is 9:1 and, by elongating the side-chain with one more methylene unit ($R^1 = CH_2CH_2Ph$), the reaction course is completely shifted towards **6f**. However, with a longer linear alkyl chain ($R^1 = CH_2(CH_2)_3CH_3$), a lower selectivity of 3.3:1 is found towards **6g**. This is in striking contrast to the substrate with $R^1 = C_6H_5$, which forms exclusively **7h** (Table 2, entry 8). However, this change in selectivity is diminished in the presence of electron-withdrawing groups in the *para* position of the aromatic system; for $R^1 = p$-CNC_6H_4, the **6i**/**7i** ratio is 1:4.5, whereas for $R^1 = p$-$NO_2C_6H_4$ the reaction towards **6j** and **7j** is almost completely unselective (Table 2, entries 9 and 10; 1.2:1).

5,6 Reaction pathway: Scope of methanobenzodioxepine scaffolds

Based on our observations of the substrate control (Table 2), we started the investigation of the scope for the formation of methanobenzodioxepines **7** by exploring the reactivity of aromatic substituted γ-keto-enals (Scheme 2). By using aldehyde **1h**, which bears a phenyl side-chain, acetal **7h** was obtained in 69% yield and 94% *ee*. 4-Chloro-1-naphthol **2b** also reacted smoothly. However, **7k** was formed in slightly lower enantioselectivity (87% *ee*), which could be solved by applying 1 mol% of the bulkier aminocatalyst **3b** (92% *ee*).

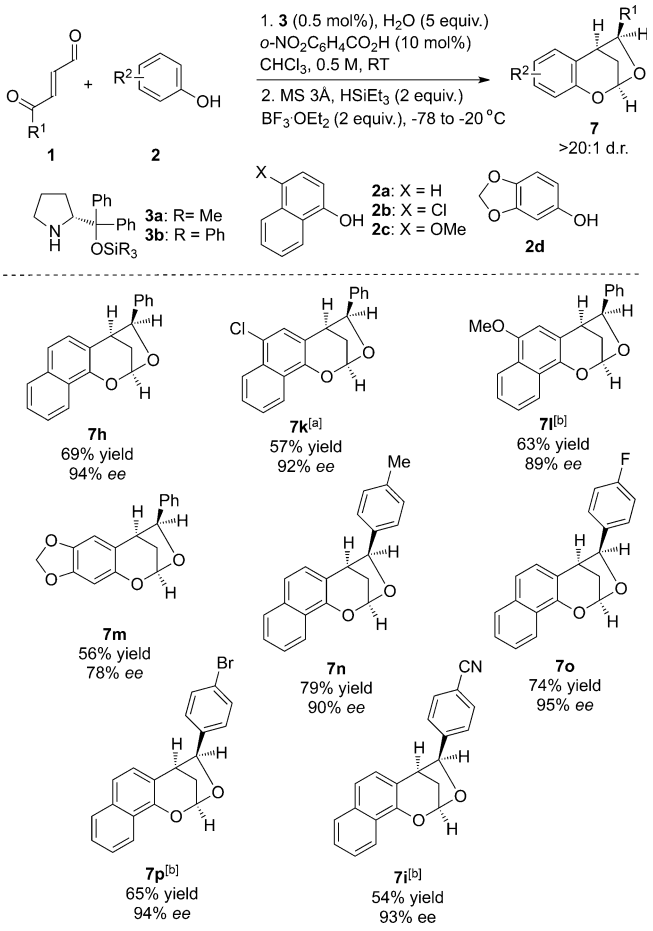

Scheme 2. Scope for the enantioselective formation of methanobenzodioxepine. Reactions were performed on a 0.25 mmol scale, with 1.5 equivalents of γ-keto-enal. Full conversion (>95%) and ratios were determined by ^{1}H NMR spectroscopy of the crude reaction mixture. [a] Reaction performed with 1 mol% of catalyst **3b**; [b] reaction performed with 0.25 mol% of catalyst **3a**.

For the reaction of the more electron-rich 4-methoxy-1-naphthol **2c**, only 0.25 mol% of catalyst **3a** was required, which afforded **7l** in 63% yield and 89% *ee*. To our delight, not only naphthols but also an electron-rich phenol reacted. When sesamol **2d** was applied as nucleophile, product **7m** was obtained in 56% yield and 78% *ee*. Unfortunately, increasing the size of the catalyst protecting group did not improve the enantioselectivity. 1-Naphthol **2a** reacted smoothly with aromatic γ-keto-enals bearing different substituent patterns, affording methanobenzodioxepines **7** in moderate to high yields (54–79%) and high enantioselectivities (90–95% *ee*). The presence of a *p*-methyl group in the aromatic moiety of the γ-

keto-enal **1k** afforded **7n** in 79% yield and 90% *ee*. Since the incorporation of a fluorine atom can change the biological properties and metabolic pathway of organic compounds,[15] we tested *p*-fluorinated γ-keto-enal **1l**, which afforded **7o** in 74% yield and 95% *ee*. When γ-keto-enals **1m** and **1i** were applied, bearing a *p*-bromo and a *p*-cyano group, respectively, only 0.25 mol% of catalyst **3a** was required. Product **7p** was isolated in 65% yield and 94% *ee*, whereas **7i** was formed in 54% yield and 93% *ee*. An aldehyde bearing a *p*-methoxy group also reacted under the reaction conditions. However, only decomposition was observed after the reduction step.

The reaction between γ-keto-enal **1h** and **2a** was scaled up to 5 mmol without observable loss in yield or enantioselectivity. The methanobenzodioxepine **7h** was isolated in 67% yield and 94% *ee*.

5,5 Reaction pathway: Scope of tetrahydrofurobenzofuran scaffolds

The scope of the formation of tetrahydrofurobenzofurans **6** from aliphatic γ-keto-enals, was also explored (Scheme 3). The chiral products were obtained in moderate to good yields (40–62%) and high enantioselectivities (84–96% *ee*).

1-Naphthol **2a** reacted smoothly with γ-keto-enals **1a**,**c**,**e**–**g**. The tetrahydrofurobenzofuran **6a** was isolated in 40% yield and 94% *ee*. By applying the bulkier aldehyde **1c**, longer reaction times were required, so 2 mol% of catalyst **3a** was applied. Product **6c** was obtained in 60% yield and 94% *ee*. When the benzyl-substituted aldehyde **1e** was used, 2 mol% of **3a** was also needed to afford product **6e** in 42% yield and 96% *ee*. For aldehyde substrates **1f** and **1g**, product **6f** was obtained in higher yield and enantioselectivity (59% yield, 95% *ee*) than **6g** (40% yield, 91% *ee*). γ-Keto-enals **1f** and **1g** also reacted with 4-chloro-1-naphthol **2b**, forming **6q** in higher yield (62% yield, 90% *ee*) than **6r** (41% yield, 89% *ee*). The reaction of benzyl-substituted γ-keto-enal **1e** with other nucleophiles also required 2 mol% of catalyst **3a**. When 4-chloro-1-naphthol **2b** was used, **6s** was obtained in 51% yield and 88% *ee*. 4-Methoxy-1-naphthol **2c** allowed the formation of **6t** in 41% yield and 92% *ee*. To our delight, sesamol **2d** also reacted, forming **6u** in 47% yield, albeit with lower enantioselectivity (84% *ee*).

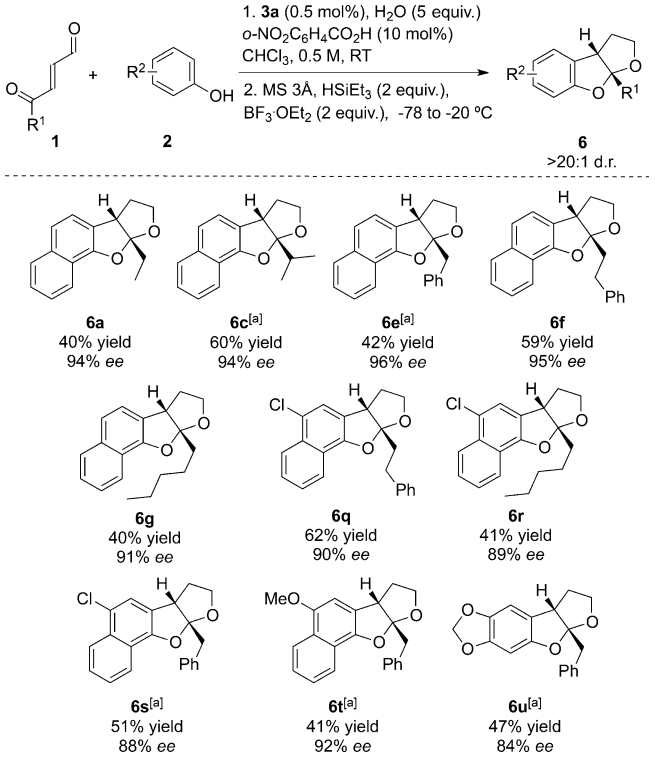

Scheme 3. Scope for the enantioselective formation of tetrahydrofurobenzofuran. Reactions were performed on a 0.25 mmol scale, with 1.5 equivalents of γ-keto-enal. Full conversion (>95%) and ratios were determined by ^{1}H NMR spectroscopy of the crude reaction mixture. [a] Reaction performed with 2 equivalents of γ-keto-enal and 2 mol% of catalyst **3a**.

2-Naphthol was also observed to react under our reaction conditions. To our surprise, this substrate seems to have a greater preference than 1-naphthol to form the 5,5-fused system over the 5,6-bridged system. However, low enantioselectivities were observed for both aldehydes bearing methyl (60% *ee*) and phenyl (44% *ee*) substituents.[14]

The absolute configuration of the benzofused acetals were unambiguously assigned by X-ray analysis of crystals of tetrahydrofurobenzofuran **6s** and methanobenzodioxepine **7k** (Figure 2).[14]

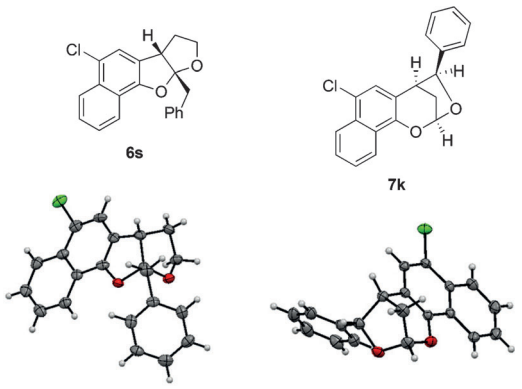

Figure 2. X-ray structures of **6s** and **7k**.

Transformations

In the previous sections, the hemiacetal moiety of intermediate **4** was reduced in all cases. To further explore the application of this functionality, γ-keto-enal **1g** and 4-chloro-1-naphthol **2b** were subjected to the optimized organocatalytic conditions and then further functionalized in a one-pot fashion (Scheme 4).[16] With BF_3·OEt_2 as Lewis acid and allylsilane as the nucleophile, the highly substituted tetrahydrofurobenzofuran **8** was obtained as a single stereoisomer in 56% yield and 90% *ee*. Furthermore, applying pyridinium chlorochromate (PCC) as oxidant led to the formation of lactone **9**, which was isolated in 37% yield and 90% *ee*.

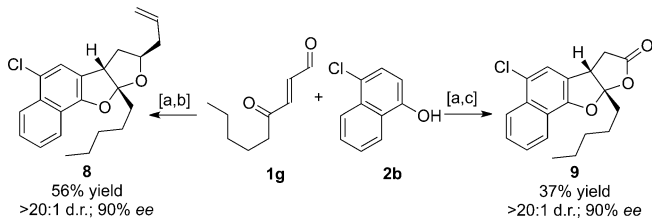

Scheme 4. Functionalizations on the tetrahydrofurobenzofuran scaffold. Reactions were performed on a 0.25 mmol scale, with 1.5 equivalents of γ-keto-enal **1g**. Full conversion (>95%) and ratios were determined by ^{1}H NMR spectroscopy of the crude reaction mixture. [a] Compound **3a** (0.5 mol%), *o*$NO_2C_6H_4CO_2H$ (10 mol%), H_2O (5 equiv.), $CHCl_3$ (0.5 M); [b] MS 3 Å (300 mg), −78 to −20 °C, BF_3·OEt_2 (2.0 equiv.), allylsilane (2.0 equiv.); [c] MS 3 Å (300 mg), PCC (2.5 equiv.).

Mechanistic insight

In Scheme 5, we propose a catalytic cycle that takes into account the observed experimental results. Assuming that water assists or accelerates the hydrolysis step, the lack of reactivity in the absence of added water suggests that the catalyst might be trapped during the course of the reaction. To support this hypothesis, stoichiometric amounts of catalyst **3a** were mixed with 4-chloro-1-naphthol **2b** and γ-keto-enals **1f** and **1h**, respectively, in $CDCl_3$ in the presence of molecular sieves. Mass spectrometry analysis of the crude reaction mixture identified the mass peaks corresponding to **10** and **11** (Scheme 5). ^{13}C NMR spectroscopy of the crude reaction mixtures revealed the presence of a carbonyl group in **10**, whereas this was not the case for **11**.[14] These observations support the proposed pathway for the formation of products **7k** and **6q**, indicating that selectivity of the reaction pathways might precede the release of the catalyst.[17] Having outlined a mechanistic proposal, our attention turned towards the investigation of the low catalyst loading required for the reaction.

With some remarkable exceptions,[18] aminocatalytic transformations often rely on relatively high catalyst loadings (10–20 mol%). The observed results for the present synthesis of benzofused acetals imply turnover numbers up to 260 (Scheme 2, **7p**), which is among the highest turnover numbers found for iminium ion-catalyzed transformations.[19] With a view to accounting for the low catalyst loadings (down to 0.25 mol%), we carried out some computational studies of the LUMO of the systems studied (Figure 3).

Although the β-carbon atom of each carbonyl group in the γ-keto-enal has equal partial positive charge, the LUMO coefficients show a polarization upon formation of its iminium ion

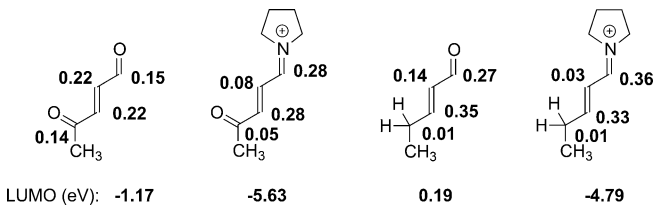

Figure 3. LUMO energies and atomic contributions (wB97XD/pcseg-1).

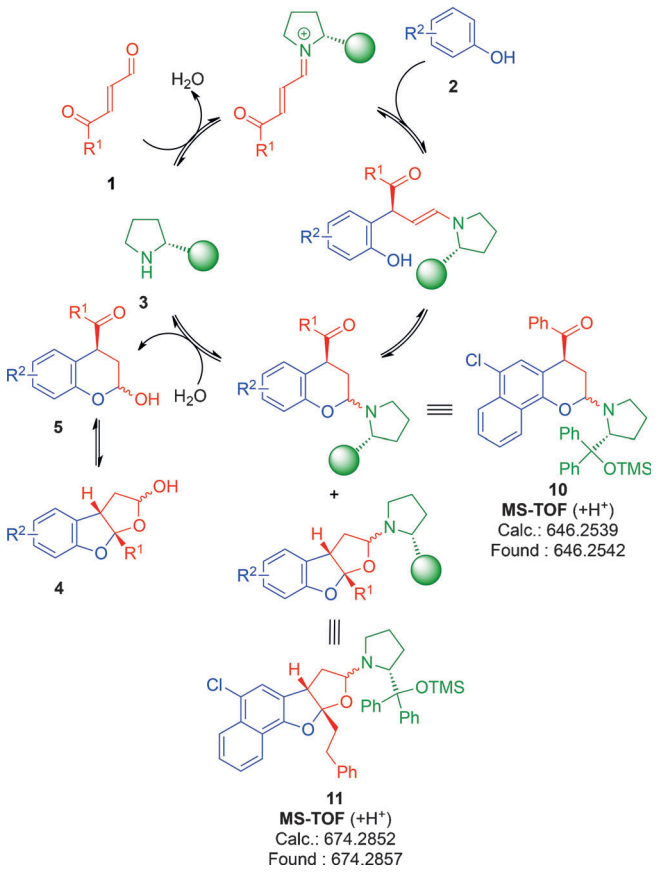

Scheme 5. Proposed catalytic cycle.

intermediate. It appears from Figure 3 that the LUMO coefficient for the β-carbon atom of the iminium ion of the γ-keto-enal is not significantly different compared to the iminium ion of pentenal. Based on frontier molecular orbital considerations, we assume that the major contribution(s) to the increased reactivity of the iminium ion system derived from the γ-keto-enal might be due to the lower LUMO energy for this system compared to the corresponding enal (Δ_{LUMO} = 0.84 eV) and/or an acceleration of the condensation step of the γ-keto-enal with the aminocatalyst compared to that of the α,β-unsaturated aldehyde (Δ_{LUMO} = 1.36 eV).

A possible explanation for the selectivity of the reaction (5,5- vs. 5,6-pathway) could arise from the relative stability of the oxocarbenium ion intermediates leading to the different products. To investigate this, we calculated the relative energies, by a composite CCSD(T) method described below, of the oxocarbenium ion intermediates (**12**–**14**) involved in the reduction steps (Table 3). The results show that the oxocarbenium ion **14** has a higher stability than the other intermediates **12** and **13** for both $R^1 = C_2H_5$ and R^1 = Ph. The effect is most prominent for R^1 = Ph, owing to the higher stabilization of a positive charge in the benzylic position on intermediate **14**.

The calculations showed that the oxocarbenium ion **14** is the most stable intermediate and thus if oxocarbenium ion formation was the rate-determining step, benzofused acetal **7** should be the only observed product for both aliphatic and ar-

Table 3. Relative energies of the oxocarbenium ion intermediates **12**–**14**.[a]

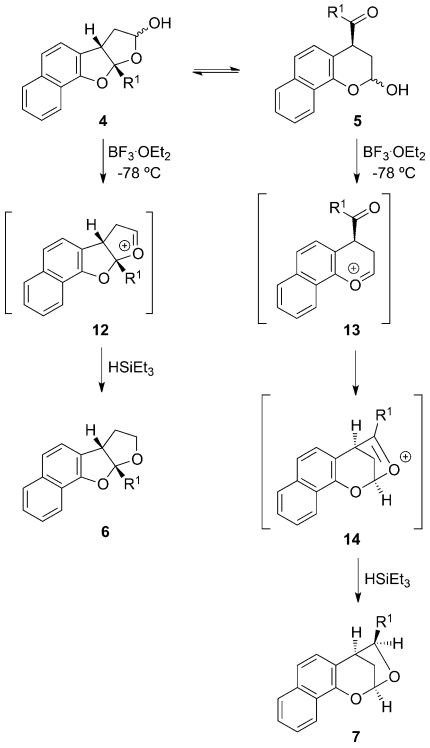

Entry	R^1	**12**	**13**[b]	**14**
1	CH_2CH_3	12.3	57.7	0.0
2	Ph	48.0	69.2	0.0

[a] Relative energies in kJ mol^{-1} obtained by a composite CCSD(T) method; [b] upon rotation of the carbonyl group, this intermediate ring-closes to **14** without an energy barrier.

omatic γ-keto-enals. However, as we observe both benzofused acetal scaffolds **6** and **7**, these results indicate that the equilibrium between the hemiacetal intermediates **4** and **5** is much slower than the reduction. Furthermore, by dissolving a crystal of **4a** in [D_6]benzene, we found that >40 h were necessary to re-establish the original equilibrium ratio between **4** and **5**, while the reduction takes 2 h at −20 °C.[14]

In an attempt to shed further light on the effects governing the equilibrium between the hemiacetal intermediates **4** and **5**, calculations of the ground-state energies of these intermediates were performed and compared with the experimentally observed product distribution of **6** and **7** (Table 4). The experimental free energies $\Delta G_{(exp)}$ (Table 4, column 1) are estimated based on the product distribution given in Table 2. The theoretical free energies $\Delta G_{(theo)}$ (Table 4, column 2) are calculated by a composite CCSD(T) method consisting of wB97XD/pcseg-1 geometry optimization of all conformations generated by the MMFF force field. Improved relative energies of the lowest conformation for each species were obtained by extrapolating MP2/cc-pVTZ and cc-pVQZ energies to the basis set limit and addition of the CCSD(T)-MP2 energy difference with the cc-pVDZ basis set. All calculations employed the $CHCl_3$ IEFPCM solvent model (IEFPCM = integral equation formalism polarizable continuum model).[20] Addition of the zero-point energy differences from wB97XD/pcseg-1 frequency calculations and Boltzmann averaging over the two diastereoisomers provided the $\Delta G_{(theo)}$ values. The ΔG values relative to those $R^1 = CH_3$ (Table 4, entry 1) are also given in Table 4 (columns 3 and 4).

Table 4. Theoretical and experimental relative free energies of hemiacetals **4** and **5** [$\Delta G = G(\mathbf{5}) - G(\mathbf{4})$].[a]

Column		1	2	3	4
Entry	R^1	$\Delta G_{(exp)}$	$\Delta G_{(theo)}$	$\Delta G_{(exp,\ rel.)}$	$\Delta G_{(theo,\ rel.)}$
1	CH_3 (**1b**)	2.1	10.5	0	0
2	CH_2CH_3 (**1a**)	5.4	11.0	3.3	0.5
3	$CH(CH_3)_2$ (**1c**)	8.7	14.4	6.6	3.9
4	$C(CH_3)_3$ (**1d**)	9.7	18.3	7.6	7.8
5	CH_2Ph (**1e**)	5.4	16.3	3.3	5.8
6	Ph (**1h**)	−7.4	3.5	−9.5	−7.0
7	*p*-CNC_6H_4 (**1i**)	−3.7	10.8	−5.8	0.3
8	*p*-$NO_2C_6H_4$ (**1j**)	0.5	12.1	−1.6	1.6

[a] Ratios were estimated based on the product distributions given in Table 2. For product **6**, the ratio also includes the amount of the open acetal form.[13]

The experimental energy differences $\Delta G_{(exp)}$ (Table 4) between isomeric hemiacetals **4** and **5** are small (0.5–9.7 kJ mol^{-1}). Figure 4 shows that the variation with substituents is reproduced with errors of a few kJ mol^{-1} (Table 4, columns 3 and 4), but the absolute values are overestimated by approximately 10 kJ mol^{-1} (columns 1 and 2). This systematic error could be due to using only the cc-pVDZ basis set for estimating electron correlation effects beyond MP2 and/or deficiencies in the IEFPCM solvent model that treats the interaction of alkyl and aryl groups with the solvent as alike.

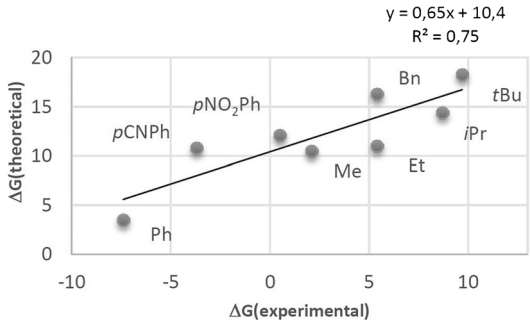

Figure 4. Correlation between experimental and computational differences in free energies (ΔG) between **4** and **5**.

To account for the different reaction pathways leading to the tetrahydrofurobenzofuran **6** and methanobenzodioxepine **7** scaffolds, a simplified explanation is suggested in Scheme 6. An initial consideration is that any effect that destabilizes **5** will shift the equilibrium towards hemiacetal **4** and vice versa. We propose a simplified model to try to account for the difference in reaction pathways. The experimentally observed conformational restrictions in propanal (Scheme 6a) are applied to try to

account for the influence of different R-alkyl substituents on the relative stability of hemiacetal **5** (Scheme 6b). For propanal, the eclipsed conformations **eclipsed-I** and **eclipsed-II** are more stable than the bisected conformations **bisected-I** and **bisected-II**. Counterintuitively, the conformation **eclipsed-I** was found to be 3.3–3.7 kJ mol^{-1} more stable than **eclipsed-II**.[21] These weak conformational preferences for **eclipsed-I** arise from stereoelectronic interactions between the σ_{C-H} and the $\pi^*_{C=O}$ orbitals of the carbonyl group (Scheme 6c).[22] The same eclipsed conformers are also calculated as the lowest energy conformation of hemiacetal **5** bearing different R-alkyl substituents (Scheme 6b).[14]

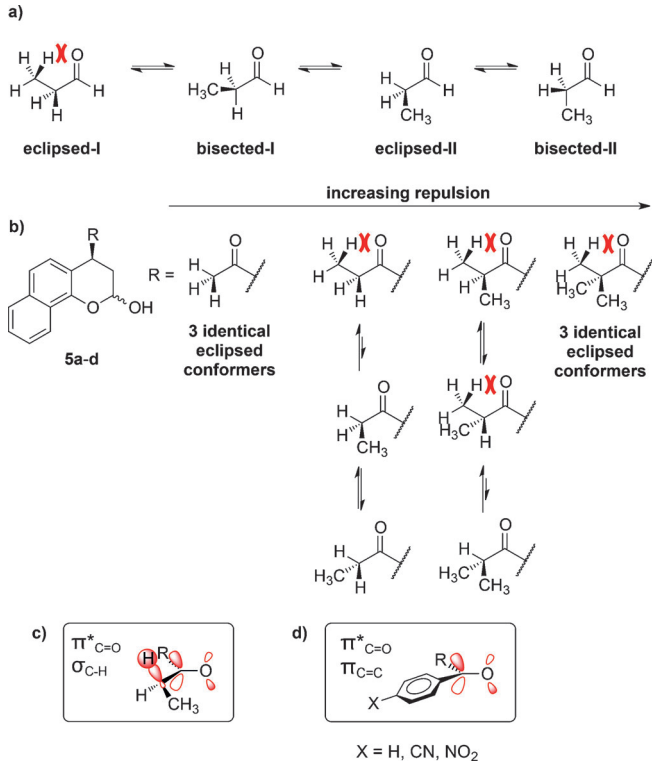

Scheme 6. Simplified models for the hemiacetal equilibrium.

This implies that, when moving along the alkyl series—methyl to *tert*-butyl—in **5**, an increase in steric repulsion between the alkyl side-chain and the carbonyl group is observed. Although the repulsion between the carbonyl and each additional methyl group might be approximately the same, the number of repulsive eclipsed conformers increases along the series. Thus, for a methyl side-chain, no such repulsion takes place, ethyl gives rise to one, isopropyl to two, and *tert*-butyl to three such repulsions, thereby increasing the overall steric interaction with the carbonyl group. This should increase the relative energy of the hemiacetal **5** when the R substituent increases in size, leading to a shift in equilibrium towards **4**. Consequently, an increased tendency towards the 5,5-reaction pathway leading to **6** should be observed, in accordance with the experimental results.

For the benzyl substituted γ-keto-enal **1e** (Table 2, entry 5), the 5,5-reaction pathway is also observed as the preferred reaction path. We suggest that **5e** behaves in a similar manner to that proposed for the alkyl-substituted substrates discussed above. However, the present simplified model seems to underestimate the selectivity for **5f** and overestimate that for **5g**. The lower predictability for **5f** and **5g** might be due to the higher degrees of freedom of the longer alkyl side-chain, which are not accounted for by the simplified model.

For the aromatic side-chains, conjugation with the carbonyl group strongly stabilizes hemiacetal **5** compared to **4**, leading to a change in the selectivity towards the 5,6-reaction pathway, providing **7** as the major product (Scheme 6d). However, the presence of an electron-withdrawing group in the aromatic ring seem to partially counter this effect as the increased electrophilicity of the keto-group shifts the equilibrium slightly towards hemiacetal **4**.[23] This effect is weakly observed for *p*-CN ($\sigma_p = 0.66$),[24] but for *p*-NO_2 ($\sigma_p = 0.78$) the reaction becomes unselective as a result of the competing effects (Table 2, entries 9 and 10).

The combined experimental and computational studies seem to account for the organocatalytic divergent 5,5- and 5,6-pathways observed for the reactions of γ-keto-enals with hydroxyarenes. These studies indicate that the distribution of the products **6** and **7** is determined prior to the reduction step by the equilibrium between **4** and **5**. This is rationalized by the reduction step being much faster than the equilibrium process. For the γ-keto-enal bearing alkyl R^1 substituents in the hemiacetal intermediate, the observed 5,5-pathway can be accounted for by a steric repulsion between the alkyl substituents and the carbonyl moiety in **5**, shifting the equilibrium towards **4**. The preference for the 5,6-pathway for the γ-keto-enal bearing aryl R^1 substituents is based on a preferred conjugation between the aromatic substituent and the $\pi^*_{C=O}$ orbital in **5**, forming **7** as the product. The calculations provided useful insights into the relatively low required catalyst loadings and the origins of the observed product distributions.

Conclusions

We have developed the first organocatalytic enantioselective syntheses of tetrahydrofurobenzofuran and methanobenzodioxepine scaffolds. The development is based on a pair of divergent pathways from hydroxyarenes and γ-keto-enals. One reaction path leads to chiral 5,5-fused tetrahydrofurobenzofuran scaffolds bearing two stereocenters, whereas the other pathway provides 5,6-bridged methanobenzodioxepine scaffolds containing three stereocenters. The tetrahydrofurobenzofurans are formed in moderate yields and up to 96% *ee*, whereas the methanobenzodioxepines are afforded in moderate to good yields and up to 95% *ee*. The reaction proceed in the presence of catalyst loadings as low as 0.25 mol%, providing one of the highest turnover numbers found in iminium ion catalysis. We applied various reactions to effect further functionalizations of the hemiacetal tetrahydrofurobenzofuran, such as reduction, oxidation and allylation. Furthermore, we studied the effects involved in the substrate control of the reaction paths, relying on both experimental and computational investigations. A simplified model based on steric, electronic,

and stereoelectronic interactions was proposed to rationalize the observed selectivities.

Acknowledgements

Thanks are expressed to Aarhus University and the Carlsberg Foundation for financial support, the CAPES Foundation and the Ministry of Education of Brazil for a predoctoral fellowship to B.M.P. (no. 9525-13-0), and the German Research Foundation (DFG) for a postdoctoral fellowship to L.K. (KL2984/1-1). Thanks are expressed to Rasmus Mose for producing the artwork.

Keywords: asymmetric catalysis · computational chemistry · fused-ring systems · organocatalysis · reaction mechanisms

[1] For representative examples, see: a) F. Perron, K. F. Albizati, *Chem. Rev.* **1989**, *89*, 1617 – 1661; b) J. E. Aho, P. M. Pihko, T. K. Rissa, *Chem. Rev.* **2005**, *105*, 4406 – 4440; c) J. A. Palmes, A. Aponick, *Synthesis* **2012**, 3699 – 3721.

[2] For a review, see: a) L. Cala, F. J. Fañanás, F. Rodríguez, *Org. Biomol. Chem.* **2014**, *12*, 5324 – 5330; for representative examples of enantioselective organocatalytic synthesis of acetals, see: b) I. Čorić, B. List, *Nature* **2012**, *483*, 315 – 319; c) M. F. Polat, L. Hettmancyk, W. Zhang, Z. Szabo, J. Franzén, *ChemCatChem* **2013**, *5*, 1334 – 1339; d) H. Huang, S. Konda, J. C.-G. Zhao, *Angew. Chem. Int. Ed.* **2016**, *55*, 2213 – 2216; *Angew. Chem.* **2016**, *128*, 2253 – 2256.

[3] G. J. Gnonlonfin, K. Hell, Y. Adjovi, P. Fandohan, D. O. Koudande, G. A. Mensah, A. Sanni, L. Brimer, *Crit. Rev. Food Sci. Nutr.* **2013**, *53*, 349 – 365.

[4] a) F. M. Talontsi, B. Dittrich, A. Schuffler, H. Sun, H. Laatsch, *Eur. J. Org. Chem.* **2013**, 3174 – 3180; b) M. El Amrani, D. Lai, A. Debbab, A. H. Aly, K. Siems, C. Seidel, M. Schnekenburger, A. Gaigneaux, M. Diederich, D. Feger, W. Lin, P. Proksch, *J. Nat. Prod.* **2014**, *77*, 49 – 56.

[5] a) G. Büchi, D. M. Foulkes, M. Kurono, G. F. Mitchell, *J. Am. Chem. Soc.* **1966**, *88*, 4534 – 4536; b) G. Büchi, D. M. Foulkes, M. Kurono, G. F. Mitchell, R. S. Schneider, *J. Am. Chem. Soc.* **1967**, *89*, 6745 – 6753; c) J. C. Roberts, A. H. Sheppard, J. A. Knight, P. Roffey, *J. Chem. Soc. C* **1968**, 22 – 24.

[6] a) A. J. Castellino, H. Rapport, *J. Org. Chem.* **1986**, *51*, 1006 – 1011; b) G. Weeratunga, S. Horne, R. Rodrigo, *J. Chem. Soc. Chem. Commun.* **1988**, 721 – 722; c) S. Horne, G. Weeratunga, R. Rodrigo, *J. Chem. Soc. Chem. Commun.* **1990**, 39 – 41; d) M. Koreeda, L. A. Dixon, J. D. His, *Synlett* **1993**, 555 – 556; e) M. C. Pirrung, Y. R. Lee, *Tetrahedron Lett.* **1996**, *37*, 2391 – 2394.

[7] G. Zhou, E. J. Corey, *J. Am. Chem. Soc.* **2005**, *127*, 11958 – 11959.

[8] a) B. M. Trost, F. D. Toste, *J. Am. Chem. Soc.* **1999**, *121*, 3543 – 3544; b) B. M. Trost, F. D. Toste, *J. Am. Chem. Soc.* **2003**, *125*, 3090 – 3100.

[9] During the preparation of this manuscript, an method capable of overcoming the substitution pattern limitation by palladium-catalyzed carboetherification was reported: G. M. Borrajo-Calleja, V. Bizer, C. Mazet, *J. Am. Chem. Soc.* **2016**, *138*, 4014 – 4017.

[10] W. Luo, Q.-S. Yu, S.-S. Kulkarni, D. A. Parrish, H. W. Holloway, D. Tweedie, A. Shafferman, D. K. Lahiri, A. Brossi, N. H. Greig, *J. Med. Chem.* **2006**, *49*, 2174 – 2185.

[11] M. A. Kamal, X. Qu, Q.-S. Yu, D. Tweedie, H. W. Holloway, Y. Li, Y. Tan, N. H. Greig, *J. Neural Transm.* **2008**, *115*, 889 – 898.

[12] For representative examples of iminium ion-catalyzed Friedel–Crafts reactions, see: a) N. A. Paras, D. W. C. MacMillan, *J. Am. Chem. Soc.* **2001**, *123*, 4370 – 4371; b) J. F. Austin, D. W. C. MacMillan, *J. Am. Chem. Soc.* **2002**, *124*, 1172 – 1173; c) N. A. Paras, D. W. C. MacMillan, *J. Am. Chem. Soc.* **2002**, *124*, 7894 – 7895; for representative examples of iminium ion-catalyzed Friedel – Crafts with naphthols, see: d) Ł. Albrecht, L. K. Ransborg, V. Lauridsen, M. Overgaard, T. Zweifel, K. A. Jørgensen, *Angew. Chem. Int. Ed.* **2011**, *50*, 12496 – 12500; *Angew. Chem.* **2011**, *123*, 12704 – 12708; e) L. Hong, L. Wang, W. Sun, K. Wong, R. Wang, *J. Org. Chem.* **2009**, *74*, 6881 – 6884; f) E. Paradisi, P. Righi, A. Mazzanti, S. Ranieri, G. Bencivenni, *Chem. Commun.* **2012**, *48*, 11178 – 11180; P. H. Poulsen, K. S. Feu, B. M. Paz, F. Jensen, K. A. Jørgensen, *Angew. Chem. Int. Ed.* **2015**, *54*, 8203 – 8207; *Angew. Chem.* **2015**, *127*, 8321 – 8325.

[13] For seminal works using diarylprolinol silyl ethers as organocatalysts, see: a) M. Marigo, T. C. Wabnitz, D. Fielenbach, K. A. Jørgensen, *Angew. Chem. Int. Ed.* **2005**, *44*, 794 – 797; *Angew. Chem.* **2005**, *117*, 804 – 807; b) Y. Hayashi, H. Gotoh, T. Hayashi, M. Shoji, *Angew. Chem. Int. Ed.* **2005**, *44*, 4212 – 4215; *Angew. Chem.* **2005**, *117*, 4284 – 4287; for a recent review, see *e.g.*: c) B. S. Donslund, T. K. Johansen, P. H. Poulsen, K. A. Jørgensen, *Angew. Chem. Int. Ed.* **2015**, *54*, 13860 – 13874; *Angew. Chem.* **2015**, *127*, 14066 – 14081.

[14] For full details, see the Supporting Information.

[15] J. Wang, M. Sánchez-Roselló, J. L. Aceña, C. del Pozo, A. E. Sorochinsky, S. Fustero, V. A. Soloshonok, *Chem. Rev.* **2014**, *114*, 2432 – 2506.

[16] For example, see: a) Y. Hayashi, *Chem. Sci.* **2016**, *7*, 866 – 880; b) L. Albrecht, H. Jiang, K. A. Jørgensen, *Angew. Chem. Int. Ed.* **2011**, *50*, 8492 – 8509; *Angew. Chem.* **2011**, *123*, 8642 – 8660.

[17] For reviews about mechanistic studies in aminocatalysis, see: a) M. Nielsen, D. Worgul, T. Zweifel, B. Gschwend, S. Bertelsen, K. A. Jørgensen, *Chem. Commun.* **2011**, *47*, 632 – 649; b) C. Moberg, *Angew. Chem. Int. Ed.* **2013**, *52*, 2160 – 2162; *Angew. Chem.* **2013**, *125*, 2214 – 2216; c) J. Burés, A. Armstrong, D. G. Blackmond, *Acc. Chem. Res.* **2016**, *49*, 214 – 222.

[18] For a review on low-loading organocatalysis, see: a) F. Giacalone, M. Gruttadauria, P. Agrigento, R. Noto, *Chem. Soc. Rev.* **2012**, *41*, 2406 – 2447; for representative examples using enamine catalysis, see: b) M. Wiesner, G. Upert, G. Angelici, H. Wennemers, *J. Am. Chem. Soc.* **2010**, *132*, 6 – 7; c) R. Martín-Rapún, X. Fan, S. Sayalero, M. Bahramnejad, F. Cuevas, M. A. Pericàs, *Chem. Eur. J.* **2011**, *17*, 8780 – 8783; d) B. Wang, X.-W. Liu, L.-Y. Liu, W.-X. Chang, J. Li, *Eur. J. Org. Chem.* **2010**, 5951 – 5954; e) X. Fan, E. Alza, M. A. Pericàs, *RSC Adv.* **2012**, *2*, 6164 – 6166; f) S. Chandrasekhar, C. P. Kumar, T. P. Kumar, K. Haribabu, B. Jagadeesh, J. Lakshmi, P. S. Mainkar, *RSC Adv.* **2014**, *4*, 30325 – 30331.

[19] For examples with low-loading iminium ion catalysis, see: a) S. Shiomi, E. Sugahara, H. Ishikawa, *Chem. Eur. J.* **2015**, *21*, 14758 – 14763; b) M.-Y. Han, H.-Z. Wang, W.-K. An, J.-Y. Jia, B.-C. Ma, Y. Zhang, W. Wang, *Chem. Eur. J.* **2013**, *19*, 8078 – 8081; c) L. Bernardi, M. Fochi, R. Carbone, A. Martinelli, M. E. Fox, C. J. Cobley, B. Kandagatla, S. Oruganti, V. H. Dahanukar, A. Carlone, *Chem. Eur. J.* **2015**, *21*, 19208 – 19222.

[20] a) J.-D. Chai, M. Head-Gordon, *Phys. Chem. Chem. Phys.* **2008**, *10*, 6615 – 6620; b) F. Jensen, *J. Chem. Theory Comput.* **2014**, *10*, 1074 – 1085; c) J. Tomasi, B. Mennuci, E. Cancès, *J. Mol. Struct. THEOCHEM* **1999**, *464*, 211 – 226; d) T. H. Dunning, Jr., *J. Chem. Phys* **1989**, *90*, 1007 – 1023.

[21] a) S. S. Butcher, E. B. Wilson, *J. Chem. Phys.* **1964**, *40*, 1671 – 1678; b) G. J. Karabatsos, H. Hsi, *J. Am. Chem. Soc.* **1965**, *87*, 2864 – 2870.

[22] O. Takahashi, K. Yasunaga, Y. Gondoh, Y. Kohno, K. Saito, M. Nishio, *Bull. Chem. Soc. Jpn.* **2002**, *75*, 1777 – 1783.

[23] H.-J. Buschmann, H. H. Füldner, W. Knoche, *Ber. Bunsen-Ges.* **1980**, *84*, 41 – 44.

[24] C. Hansch, A. Leo, R. W. Taft, *Chem. Rev.* **1991**, *91*, 165 – 195.

Received: June 23, 2016
Published online on ■■ ■■, 0000

FULL PAPER

Organocatalysis

*B. M. Paz, L. Klier, L. Næsborg, V. H. Lauridsen, F. Jensen, K. A. Jørgensen**

■■ – ■■

Enantioselective Organocatalytic Cascade Approach to Different Classes of Benzofused Acetals

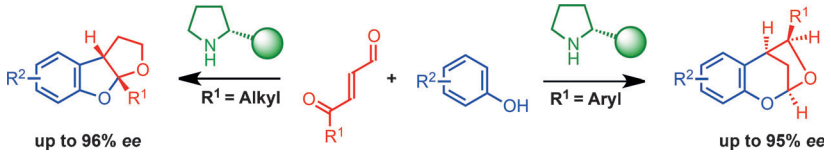

Different class: A novel enantioselective organocatalytic strategy is presented for the synthesis of tetrahydrofurobenzofuran structures, based on a pair of divergent reaction pathways in which hydroxyarenes react with γ-keto-α,β-unsaturated aldehydes, catalyzed by a chiral secondary amine. The reaction is remarkable as it proceeds with catalyst loadings as low as 0.25 mol%.

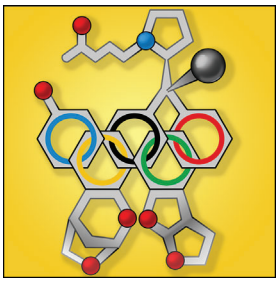

Cascade Synthesis

In their Full Paper on page ■■ ff., K. A. Jørgensen et al. present a novel enantioselective strategy for the synthesis of tetrahydrofurobenzofuran and methanobenzodioxepine structures, based on a pair of divergent reaction pathways in which hydroxyarenes react with γ-keto-α,β-unsaturated aldehydes, catalyzed by a chiral secondary amine. One reaction pathway leads to chiral 5,5-fused acetals, the tetrahydrofurobenzofuran scaffolds, with two stereocenters, whereas the other reaction pathway provides 5,6-bridged methanobenzodioxepine scaffolds with three stereocenters. The reaction can proceed with catalyst loadings as low as 0.25 mol%, giving among the highest known turnover numbers in iminium ion catalysis.